

Experimental investigation of the turbulent cascade development by injection of single large-scale Fourier modes

Margherita Dotti · Rasmus K. Schlander · Preben Buchhave · Clara M. Velte

Received: date / Accepted: date

Abstract The current work presents an experimental investigation of the dynamic interactions between flow scales caused by repeated actions of the nonlinear term of the Navier-Stokes equation. Injecting a narrow band oscillation, representing a single Fourier mode, into a round jet flow allows the measurement of the downstream generation and development of higher harmonic spectral components and to measure when these components are eventually absorbed into fully developed turbulence. Furthermore, the dynamic evolution of the measured power spectra observed corresponds

Financial support from the Poul Due Jensen Foundation (Grundfos Foundation) for this research is gratefully acknowledged. Grant number 2018-039.

M. Dotti
Department of Mechanical Engineering, Technical University of Denmark, Nils Koppels Allé, Bldg. 403, 2800 Kgs. Lyngby, Denmark.

E-mail: mardott@kt.dtu.dk *Present address:* Department of Chemical and Biochemical Engineering, Technical University of Denmark, Søtofts Plads 228A, 2800 Kgs. Lyngby, Denmark

R.K. Schlander
Department of Mechanical Engineering, Technical University of Denmark, Nils Koppels Allé, Bldg. 403, 2800 Kgs. Lyngby, Denmark.

E-mail: rasmuskorslund@gmail.com *Present address:* Department of Aeronautics, Imperial College, London SW7 2AZ, United Kingdom

P. Buchhave
Intarsia Optics, Sønderkovvej 3, 3460 Birkerød, Denmark.
E-mail: buchhavepreben@gmail.com

C.M. Velte
Department of Mechanical Engineering, Technical University of Denmark, Nils Koppels Allé, Bldg. 403, 2800 Kgs. Lyngby, Denmark.
ORCID: 0000-0002-8657-0383
E-mail: cmve@dtu.dk

well to the measured cascaded delays reported by others. Closely matching spectral development and cascade delays have also been derived directly from a one-dimensional solution of the Navier-Stokes equation described in a companion paper. The results in the current work provide vital information about how initial conditions influence development of the shape of the spectrum and about the extent of the time scales in the triad interaction process, which should be of significance to turbulence modelers.

Keywords Turbulence cascade · Triad interactions · Laser Doppler Anemometry · Hot-wire Anemometry · Velocity Power Spectrum · Turbulence modeling parameters

1 Introduction

Most of the 20th century knowledge of turbulence is founded on the equilibrium gas dynamics analogy to small and intermediate scales of turbulence, as put forth by Kolmogorov [1, 2]. Indeed, almost all turbulence theories and models are in one way or another based on the Kolmogorov theory of turbulence (which the authors will hereafter refer to as the K41 theory). In particular, many approaches rely on the existence of a continuous exchange of turbulent energy from small to large wave numbers, the Richardson cascade, where predominantly local interactions between scales are assumed to occur [2, 3, 4].

By taking the Fourier transform of the non-linear advection term in the Navier-Stokes equation, one can immediately observe the possibilities of energy transfer between different wavenumbers of the velocity field. However, being able to infer the restriction of locality of the triad interactions, as postulated by Richardson,

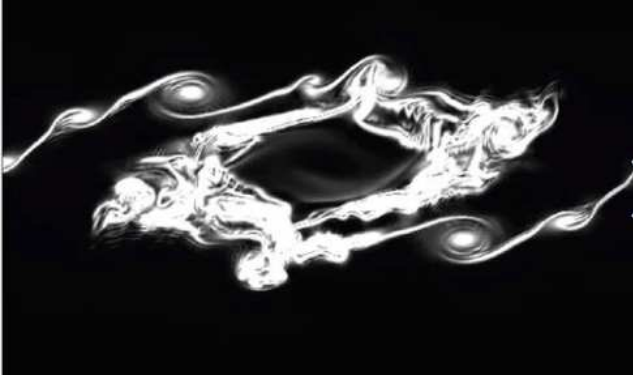


Fig. 1 Generation and interaction of non-local scales [5].

directly from the governing equations appears to have so far eluded the turbulence community. On the other hand, accumulating evidence witnesses that the actual underlying processes of energy exchange between scales may in fact be quite different from the ideas of K41. An example of non-local energy exchange, in direct violation of the Richardson cascade concept, is shown in Figure 1 [5]. This figure zooms into a shear layer, from a Direct Numerical Simulation (DNS) computation, where structures of small size appear and directly exchange energy with significantly larger structures.

Historically, much (but not all) of the published experimental evidence supported the K41 theory. However, George [6], inspired by recent developments of his and others, argued that the K41 only applies to equilibrium flows, while failing to reproduce results from flows out of equilibrium.

Recently, interesting dynamic effects in the transfer of turbulent energy by the triad interaction process have been reported. For instance, the data of the hot-wire anemometer analysis conducted by Josseland *et al.* [7] reveals both a lack of time reversal symmetry and a delay in the triad interactions. This delay seems to depend on the separation of the k -vectors entering the process. Other relevant studies concern the comparison between the strength of non-local interactions against the local ones [8,9] and the persistence of the initial large-scale structures during the further turbulence development [10]. As Zhou [8] pointed out, and several investigations concluded, the local energy transfer resulted from non-local interactions [11,12,13], which contrasts with the classical Kolmogorov picture.

Indeed, direct coupling between scales of quite different size seems to be possible [14], as is also shown in Figure 1. And even though the net effect of the energy transport is towards higher wavenumbers, the energy may move in the direction of both smaller and larger scales. Other outstanding questions concern the persistence [15] of the initial conditions into the de-

veloped turbulence and the precise form of the final decay of the turbulent fluctuations [16]. Moreover, the fact that many papers report deviations from the $-5/3$ slope in turbulence velocity power spectra [14,17,18,19] and that significant differences occur between measurements and model calculations in flows of significant stagnation, separation and transient processes (i.e. where the flows can potentially be pushed out of the assumed equilibrium) highlight the need for investigations that go beyond the Kolmogorov theory. For this reason, the authors believe that the turbulence energy transfer investigation should refer directly to the governing Navier-Stokes equation [20].

The current work describes an attempt to isolate and visualize triad interactions and their dynamics by measuring the downstream development of a single or a few Fourier components, here performed as narrow-band temporal and spatial oscillations, injected into a well-defined flow. The downstream position is interpreted as a time development, given by the convection time for a fluid element, in which the fluid has been exposed to the actions of the Navier-Stokes equation. The triad interaction mechanisms have been generated and isolated by inserting an oscillation into a mean flow direction with two different methods. The measurements have been compared with the flow development simulated by a one-dimensional solution of the Navier-Stokes equation, which is described in more details in the companion papers [20,21]. The present work shows good agreement between the experiments and the computations and conclusions are drawn based on the resulting dynamics of the initial mode injection.

2 Navier-Stokes equation

The Navier-Stokes equation is a three-dimensional description of the time evolution of fluid flow. The equation is essentially the application of Newton's second law to the motion of fluid passing through an infinitesimal fluid control volume, as shown in Figure 2.

The development of the flow structures and the interchange of energy between them is primarily caused by the non-linear term in the Navier-Stokes equation. This nonlinear term causes a variation in velocity, due to the change in convection of momentum through a control volume, $CV = dA \cdot ds$, where dA is the cross-sectional area and ds is the thickness of the CV . The viscous diffusion term causes a loss of velocity by diffusion of momentum to the fluid surrounding the control volume.

The pressure gradient influences the velocity by fluctuating (dynamic) pressure caused by velocity fluctuations elsewhere in the fluid and propagating instan-

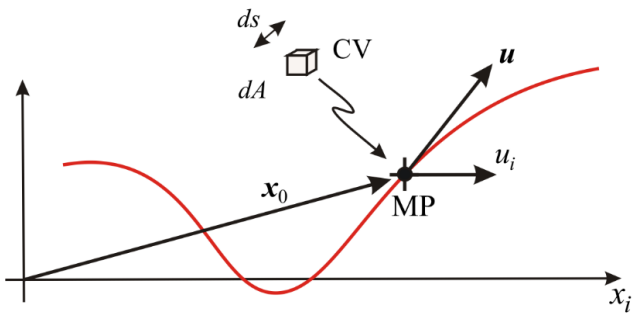


Fig. 2 Fluid control volume and instantaneous velocity u and a component u_i at a point in space-time. The red line indicates a streak line.

taneously to the control volume in an incompressible fluid. This term must be computed by a full solution to the Laplace equation including pressure terms at the boundaries or inferred from theoretical models. Thus, the equation is local, describing the conditions at a ‘point’, non-local effects only entering through pressure effects created by velocity fluctuations or through boundary conditions elsewhere in the fluid, transmitted to the point of interest.

The velocity field may be decomposed in several ways, for example by analyzing the triad interactions between the Fourier coefficients or wave vector components of the flow. If one includes time in the decomposition [6,20], it can be seen that the phase match condition is extended beyond the classical one between three wavenumber vectors, $\mathbf{k} = \mathbf{k}_1 + \mathbf{k}_2$, to one that includes also frequency and time, $[\mathbf{k} - (\mathbf{k}_1 + \mathbf{k}_2)] \cdot \mathbf{r} - [\omega - (\omega_1 + \omega_2)] t = 0$. A mismatch in the wavenumbers, $\Delta\mathbf{k} = \mathbf{k} - (\mathbf{k}_1 + \mathbf{k}_2)$, can therefore be compensated by a mismatch in the frequencies, $\Delta\omega = \omega - (\omega_1 + \omega_2)$. This can give rise to time delays in the interactions introducing dynamics into the classical triad interactions analysis [9].

Several experiments have been designed to explore the underlying wave interaction dynamics: In the first experiment, an actual narrow-band oscillating velocity, that resembles a single Fourier mode, is injected into a fully developed turbulent jet flow. By conducting measurements downstream of the injection position, the development in time of the power spectrum is traced through laser Doppler anemometry (LDA) and hot-wire anemometry (HWA) measurements. The downstream position is interpreted in relation to the Navier-Stokes equation as a time interval in which the equations operate on the flow passing a series of control volumes, as shown in Figure 2. Tests of zither-like grid generated modes were performed as early as 1980 [23], and detailed studies of full and narrow-band velocity correlations in wind tunnel flow was made as early as 1971.

However, the clear evolution of the spectrum that we report here has not been reported before.

A ‘full’ solution to the Navier-Stokes equation requires a four-dimensional numerical solution with a high spatial and temporal resolution (DNS). However these numerical solutions do not necessarily provide a physical understanding, i.e., the comprehension of the flow based on the governing equations, which is the primary interest in the current work. Therefore, to understand the inner workings of the interactions between Fourier components (the triad interactions), a one-dimensional model has been developed and implemented [21]. The method involves projection of the forces acting on the fluid in the control volume onto the instantaneous velocity direction. The time sampling interval Δt is then converted to the convection sampling interval $\Delta s = u\Delta t$ [24]. This method, obviously, does not allow to see the full 4-dimensional motion of the fluid. However, the forces acting in the direction of the velocity will change the momentum and allow computation of kinetic energy and spatial velocity structures. The main problem is the inability of computing the pressure gradient, since this requires the solution of Laplace’s equation for the whole fluid volume at the present instant in time. To include pressure, it will be necessary to invoke a model or use separate information about the fluctuating pressure.

3 Experiments

The experiments described in the following are designed to inject a single Fourier mode into a well-defined flow and by measurement of the time trace along the downstream evolution follow the time development of the velocity field. As Fourier modes are essentially plane waves [26], the attempt was to inject a two-dimensional oscillating wave front developing along the mean flow direction.

The axisymmetric turbulent round jet can be considered ideal to investigate the turbulent cascade. Indeed, the round turbulent jet was the first flow for which the theory of Kolmogorov was supported by showing the $-5/3$ range in the power spectrum [27]. In addition, this flow evolves rapidly enough to be practical on laboratory scales, and it is optically accessible. Moreover, it offers a useful wide literature, as it has been investigated by many over the years, see e.g. [28,29,30,31].

The measurements are divided in three sets of experiments, presented in chronological and thought chain order, and were carried out using a laser Doppler anemometer and a hot-wire anemometer. First, LDA measurements were performed behind an oscillating airfoil designed to inject a single frequency oscillation into a high

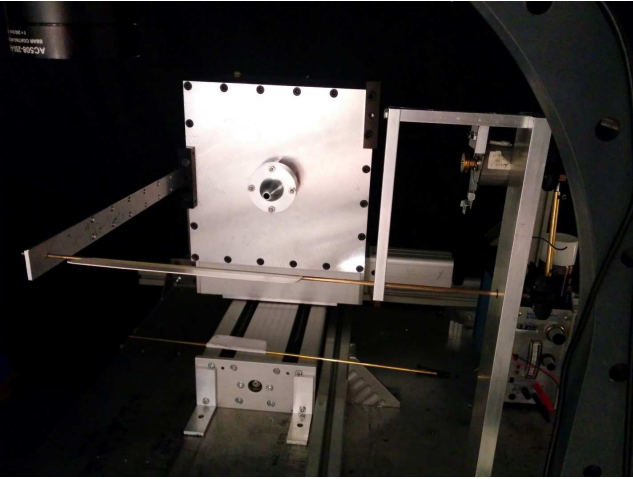


Fig. 3 Jet generator and oscillating airfoil.

intensity turbulent round jet flow. Secondly, measurements in jet flows of different Reynolds numbers from the same jet facility were carried out behind a larger airfoil with less vigorous oscillations using a hot-wire anemometer. Finally, the same hot-wire anemometer system was used to measure vortex shedding in a low intensity turbulent jet of significantly larger jet exit diameter, employed as an open wind tunnel. This third experiment was performed in the laminar jet core using a sharp-edged rod to create a distinct vortex shedding frequency.

3.1 Oscillations in turbulent jet – small airfoil (LDA)

A jet generator, which is the one used in several projects of the Turbulence Research Laboratory of DTU [31, 32, 33], produces an axisymmetric fully developed turbulent flow 30 jet exit diameters downstream of the nozzle exit. The jet nozzle, shown in Figure 3, has an exit diameter of $D = 10\text{ mm}$, a contraction ratio of 3.2 : 1 and can be moved in two horizontal directions, manually or by computer control. The jet is connected to a pressurized air output, used to adjust the flow velocity, and to a particle dispenser that seeds the flow. The nozzle was designed using a fifth order polynomial contraction shape as suggested by [34] in order to avoid boundary layer separation at the walls and to obtain a uniform mean flow at the outlet.

The airfoil altered the jet flow by introducing a strong sinusoidal frequency. This airfoil was situated 20 jet exit diameters downstream of the jet exit at the height of the nozzle centerline and extended through the full width of the jet, as depicted in Figure 3. Figure 4 shows a smoke visualization using a vertical laser sheet across the streamwise development, illustrating the jet



Fig. 4 Flow visualization airfoil experiments.

flow perturbed by the airfoil. Initially, the airfoil span experiment was conducted by flapping in an oscillating manner a $50 \times 10\text{ mm}$ airfoil with a thick leading edge and a sharp trailing edge.

The airfoil was actuated by a small motor, creating an oscillation frequency of 10 Hz . The streamwise velocity component was measured using an in-house state-of-the-art side scatter LDA system [32]. Since the side scattering optics of the LDA system was highly sensitive to misalignments, it was decided to traverse the jet instead of the LDA system. The measuring distance was 300 mm and the size of the measurement volume was, due to the side scattering configuration, nearly spherical with a diameter of $200\text{ }\mu\text{m}$. When performing LDA measurements, the ambient air was seeded with glycerin particles, injected by means of pressurized air, so that a nearly uniform spatial seeding density is achieved. The size of the scattering particles ($\sim 1 - 5\text{ }\mu\text{m}$) has been shown to be small enough to faithfully track the flow and observed to be large enough to scatter enough light for a to produce a satisfactory signal quality [35]. The Doppler signal at each downstream position was measured in 400 records, each of 2 s , with a sampling rate of 25 MHz . The Reynolds number at the jet exit was $Re_D = U_0 D / \nu = 2.2 \cdot 10^4$. The LDA measurement volume was then placed at 1D, 2D, 4D, 6D, 8D, 10D jet diameters downstream from the trailing edge of the airfoil, as depicted in Figure 5.

The corresponding measured temporal streamwise velocity power spectra are displayed in Figure 6. The sequence of plots shows interesting dynamics in the energy exchange process between scales. Energy tends to be exchanged between harmonics of the base frequency of 10 Hz , which is well in line with the fact that the non-linear term in the Navier-Stokes equation introduces frequency doubling, sum- and difference-frequencies as

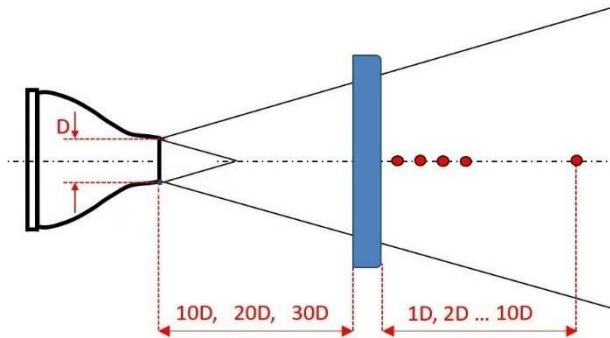


Fig. 5 Schematic (not to scale) of the setup of the oscillating airfoil in a turbulent jet. The airfoil is depicted in blue and the measurement points in red.

shown analytically in [21]¹. From the figure it can also be inferred that the center of gravity of the induced spectral peaks moves towards higher frequencies as the flow is traced downstream. The alternation of the dominance of the first (10 Hz) and second (20 Hz) harmonic, the ‘wave behavior’, is in agreement with Josserrand *et al.* [7], who observed that energy transfers primarily among wavenumbers which are strongly correlated to the fundamental frequency. Moreover, it shows that the energy can flow in both directions, but the global energy transfer remains towards higher frequencies.

3.2 Oscillations in turbulent jet – large airfoil (HWA)

The LDA measurements and flow visualization from the previous section showed that the $50 \times 10\text{ mm}$ airfoil required a significant amplitude to create the desired modulation to ensure injection and isolation of the development of a single mode into the jet. Thus, new measurements were conducted with a larger (span and chord) airfoil, which was oscillating with a smaller amplitude to introduce less energy. The dimension of both the chord and the span dimension of the airfoil was increased to 50 and 210 mm, respectively. A hot-wire anemometer could, to sufficient accuracy, be used in this less turbulent flow because the power spectrum could be processed online, and the system could be more easily traversed to cover more downstream measurement points.

A Mini CTA 54T30 system for measurements in air from Dantec Dynamics was used for acquisition. The 55P11 straight single wire probe (Tungsten, $d = 5\ \mu\text{m}$ and length 1 mm) was connected through the straight 55H20 support through a 4.0 m cable. Calibration was

¹ This is easily observed e.g. by substituting a velocity wave traveling in the x-direction $u(x) = U \cos(k_x x)$ into $(\mathbf{u} \cdot \nabla)\mathbf{u}$

performed across 10 velocity points, from 1 ms^{-1} to 30 ms^{-1} and measuring the pressure difference with an FCO560 Furness Anemometer. The record length of each measurement was set to 120 s and each signal was sampled with a rate of 30 kHz. The data was transferred to a computer passing through an anti-aliasing filter and processed with the Dantec MiniCTA v4.05 software. The oscillating airfoil was positioned with its leading edge at 10, 20 and 30 jet exit diameters, respectively, downstream of the jet exit and different Reynolds number flows were tested. The velocity was measured at several positions downstream from the airfoil trailing edge until the point where the injected mode was fully absorbed into the background turbulence of the jet.

An example of the hot-wire measurement results is displayed in Figure 7. This experiment was carried out at $Re_D = 4.7 \cdot 10^4$, keeping a distance of $10D$ between the jet exit and the leading edge of the airfoil. The spectra were measured at increasing axial distances between $1D$ and $50D$ from the airfoil trailing edge. These spectra are displayed in one graph with an offset of 10 – 15 dB between each for the sake of comparison of the peaks.

Several features of this plot are noteworthy. It can be observed that the low order harmonics are created at an early stage, and several frequencies are observed already close to the trailing edge of the flap; note that the closest practical position of measurement was $1D$ from the airfoil trailing edge. Note that the third harmonic remains weaker than higher harmonics across the full downstream development. This phenomenon is explained in a companion paper [20] as a result of the finite region for the interaction of the participating Fourier components. The spectral window, caused by the finite interaction region, modifies the shape of the spectrum in comparison to a spectrum created in an infinite region. Furthermore, the generation of the third harmonic in particular requires the prior creation of the 2^{nd} harmonic in order to take place [20].

Figure 7 shows that the energy associated with the injected frequency of 10 Hz depletes downstream, while the 20 Hz second harmonic peak initially increases and subsequently decreases after reaching its maximum around approximately $8D$. A similar behavior can be seen for the higher harmonics. The energy of the generated peaks eventually becomes absorbed in the developed turbulence further downstream. This behavior is analogous that depicted in Figure 6: the transfer of energy can be both direct and indirect, but the net effect shifts the concentration of energy towards higher frequencies [20, 21].

The striking stability and sharpness of the higher harmonics in Figure 7 is noteworthy. Even at the late stages just before being absorbed, the positions of the

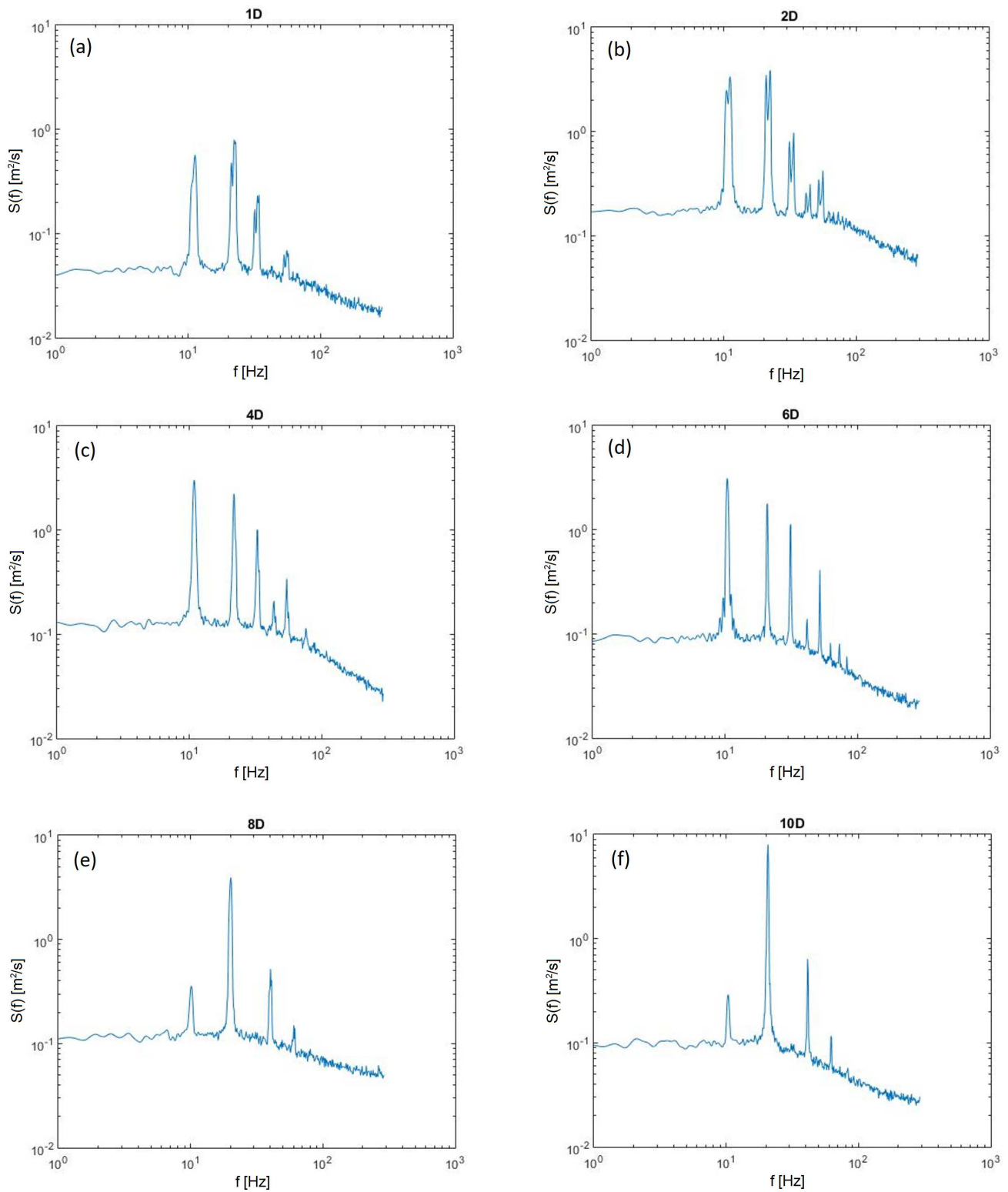


Fig. 6 Dynamic evolution of a ‘wave-like behavior’ of the spectral harmonic peaks for distances of $1D$, $2D$, $4D$, $6D$, $8D$ and $10D$ behind the airfoil trailing edge, respectively.

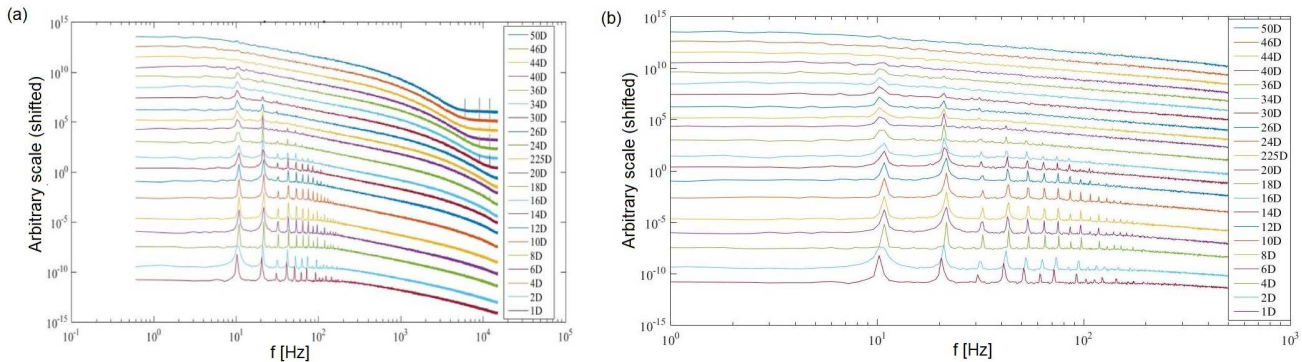


Fig. 7 Downstream spectrum development for $Re_D = 4.7 \cdot 10^4$ and $10D$ between the jet exit and the airfoil leading edge. (a) Full view and (b) zoom-in on the peak development.

Table 1 Reynolds number dependence of the time for absorption of the spectral peaks.

Re_D	Absorption time [s]
$2.2 \cdot 10^4$	0.1694
$3.0 \cdot 10^4$	0.1343
$3.6 \cdot 10^4$	0.1124
$4.2 \cdot 10^4$	0.0944
$4.7 \cdot 10^4$	0.0902

peaks remain at their precise integer values of the airfoil excitation frequency and are apparently not smeared out by the surrounding, presumed Stochastic, turbulent velocity fluctuations. This behavior may partly arise due to the fact that the injected mode is characterized by a much larger energy than the ones relative to the general turbulence. Consequently, the interaction between harmonics wavenumbers remains more efficient, leading to the persistence of the initial structure far downstream in the jet (historically referred to as ‘permanence of large eddies’). This result lends strong support to the ideas of turbulence dependency upon initial conditions (in contrast to assuming universality), in line with our recent results [19,20,21].

The time for absorption of the peaks in Figure 7 and corresponding parametric experimental investigations can be found from the integration of the downstream decaying velocity over the downstream distance. The results are summarized in Table 1. The absorption time of the peaks, which should be of significance to turbulence modelers, depends in the current case on the Reynolds number. In this regard, it has been noticed that the peaks are, independently of Reynolds number, consistently completely absorbed around approximately the same downstream spatial position, i.e. $\sim 44D$ after the trailing edge of the airfoil. This appears to be independent of the fact that the peaks from the non-linear interactions are more pronounced for higher Reynolds numbers.

3.3 Vortex shedding in laminar jet core (HWA)

Vortex shedding measurements were also carried out in the laminar core of a round turbulent jet with exit diameter $D = 100 \text{ mm}$ and contraction ratio $2.4 : 1$. The jet could in this manner serve as an open wind tunnel with a nearly uniform exit velocity profile. The velocity can be determined from the pressure drop across the nozzle. A distinct vortex shedding frequency is injected into the laminar jet core by positioning a sharp-edged vertical rod at the nozzle outlet. The rod had a cross-section of $10 \times 2 \text{ mm}$. As Figure 8 shows, the rod span extends across the entire nozzle diameter.

The objective was to isolate the workings of the non-linear term by isolating the downstream development of a sharply defined Fourier mode injection using a shedding generator. This allowed for measurement of the very initial generation as well as the downstream development of the triadic interactions. This was not possible with the oscillating airfoil generated shedding, since measurements were only practical just behind the flap trailing edge where the energy distribution had already had ample time to develop across the airfoil chord. This setup, on the other hand, allows measurements from even the initial generation of the base frequency.

In Figure 9 a flow visualization of the flow behind the vertical rod is shown. The laminar jet core around the sharp-edged rod is clearly visible in Figure 9 along with the Kelvin-Helmholtz vortices developing farther downstream. Downstream of the rod, the flow vortex shedding formed by the sharp edge imposes a single fundamental frequency.

The same hot-wire anemometer system from Dantec Dynamics, as described previously, was employed. For the current experiment, the signal was captured using a PicoScope 5444B by Pico Technology. This scope allowed the change in both the waveform signal and the flow spectrum to be visualized in nearly real time,

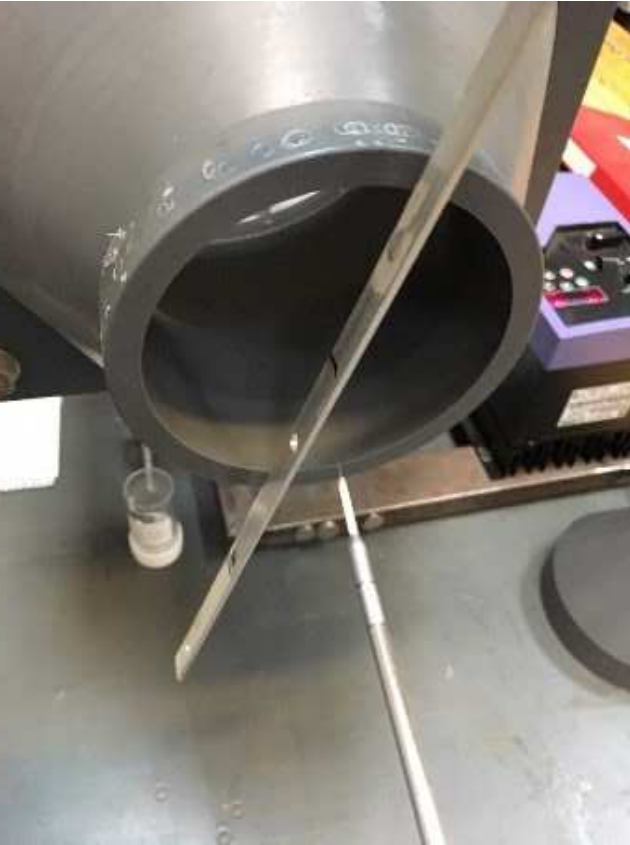


Fig. 8 Jet with an extended laminar core, flat rod and hot-wire anemometer probe.

allowing therefore to quickly find identify the desired measurement points. The measurements were acquired with 0.5 mm intervals from 0.5 mm to 10 mm downstream from the vertical rod at $Re_D = 1.06 \cdot 10^4$. Figure 10 depicts a schematic of the linear region of the acquisition positions (in blue) from a top and a side view, respectively. The spanwise position was kept fixed to a distance of 1 mm from the rod edge.

A total of 100 time-series of 0.2 s each were acquired in each measurement point with a sampling rate of 20 kHz , a hardware resolution of 12 bits and sampling interval $50\text{ }\mu\text{s}$. A spectrum was produced for each spatial point, cutting out the DC part of the signal and employing a Hamming window function, with a range of 50 kHz . A computer simulation applying a one-dimensional projection of Navier-Stokes equation onto the instantaneous flow direction is reported in [20]. The program assumes a time record of the velocity as input and computes the time development of the velocity trace employing multiple incremental passes through a fluid control volume exposed to the effect of the terms in the Navier-Stokes equation.

One result from this calculation is quoted and compared to one of the measurements. The measured time

trace from the spatial point closest to the rod has been used as input to the computer program, so that the initial condition for the development of the velocity in the flow is identical to the initial velocity trace used in the program. The program uses a rectangular low-pass filter, which cuts out the DC part of the signal and some high frequency peaks due to external noise on the time traces. The spectra are then computed employing a Hamming window function, just like the PicoScope does. Note, the program uses only the terms in the Navier-Stokes equation without further approximations.

Figure 11 reports the downstream evolution of the experimental (blue) and the computational (red) downstream dynamic power spectra. The links in the figure captions provide moving images displaying the downstream evolution of the repeated workings of the non-linear term on the initial modal injection. Note that the acquisition instrument introduces a filter, manifesting itself as a slow variation across frequency, which should be disregarded when interpreting the results.

The plots in Figure 11(a) and 11(b) display respectively the first spectrum measured close to the vortex shedding rod and the spectrum measured at a distance of 10 mm downstream. Figures 11(c) and 11(d) display the corresponding results from the simulation. From these results, the delays in the cascade wavenumber interactions are particularly evident. Indeed, in contrast to Figure 7, where the low order harmonics are already present even in the most upstream measurement, in Figure 11 only the initial peak is present at the initial measurement point.

The time scale for vortex shedding to develop and reach an ‘asymptotic’ configuration (like the one shown in Figure 11b) has been computed for the considered experiment and was found to be 6 ms . The time was estimated from the integration of the downstream velocity over the downstream distance, as for the time for absorption of the peaks of Table 1.

4 Conclusions

The energy transfer between different scales of velocity fluctuations is a key process in the development of turbulence, and knowledge of the efficiency and time scales for these energy exchanges is crucial for the understanding of turbulence theory and for further development of engineering models. The exchange between harmonics of the originally injected frequency is well in line with the fact that frequency doubling and sum- and difference-frequencies are to be expected as a result of the actions of the nonlinear term of the Navier-Stokes equation [21].



Fig. 9 Vortex shedding flow visualization.

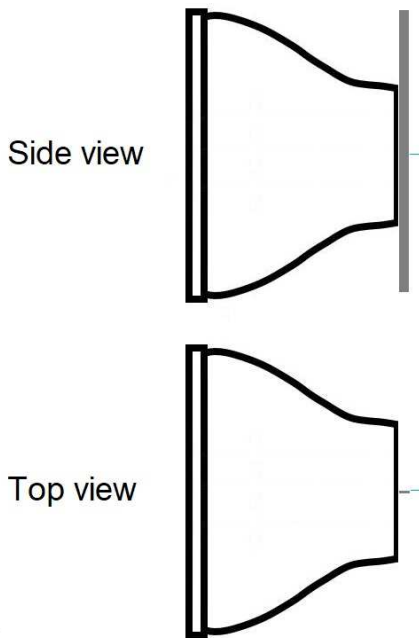


Fig. 10 Schematic (not to scale) of the vortex shedding experiment in a laminar jet core, including the sharp-edged rod (in grey) to inject a sharp frequency and the region of the measurement points (indicated by a blue line).

Three experiments were performed where a single Fourier mode was injected into a well-defined turbulent flow and the development of the velocity power spectrum was traced along the downstream direction. The downstream convection has been considered as a successive exposure of the initial velocity trace to the Navier-Stokes equation in a small fluid control volume. This point of view allowed us to compare the development of the measured spectra to the spectra computed by a one-dimensional computer simulation with the measured initial time trace as input and to compute the power spectra as this time trace was transformed

by incremental repeated exposures to the Navier-Stokes equation.

Although the particular form of the measured and computed power spectra depends on the initial position of the measurement point and the way the Fourier mode was injected, a number of common properties were revealed:

- Higher order frequency components were formed successively as a fluid element passing near the point of injection evolved downstream in time.
- The higher frequencies were exact multiples of the injected frequency and they retained their well-defined sharp spectral frequency – even when submerged into high-intensity turbulence.
- Far downstream the spectrum tends to an asymptotic form whose energy is slowly being absorbed into the surrounding turbulence.
- The absorption distance does not change significantly with Reynolds number in the investigated range $Re = 22.000 - 47.000$. The absorption time, consequently, varies with Reynolds number (jet exit velocity).
- The transfer of energy between modes is seen to be both direct and indirect, but it occurs predominantly from low wavenumbers towards higher wavenumbers.
- A delay in the interactions between the injection harmonics is evident in all experiments. The initial development is particularly carefully isolated in the measurement of the vortex shedding from a sharp-edged rod in a laminar jet core.
- Influence of the initial spectral components on the far downstream spectrum is clearly evident, in particular in the oscillating airfoil measurements in a turbulent jet.

All in all, the measurements and computer simulations illustrate the dynamic nature of the triadic inter-

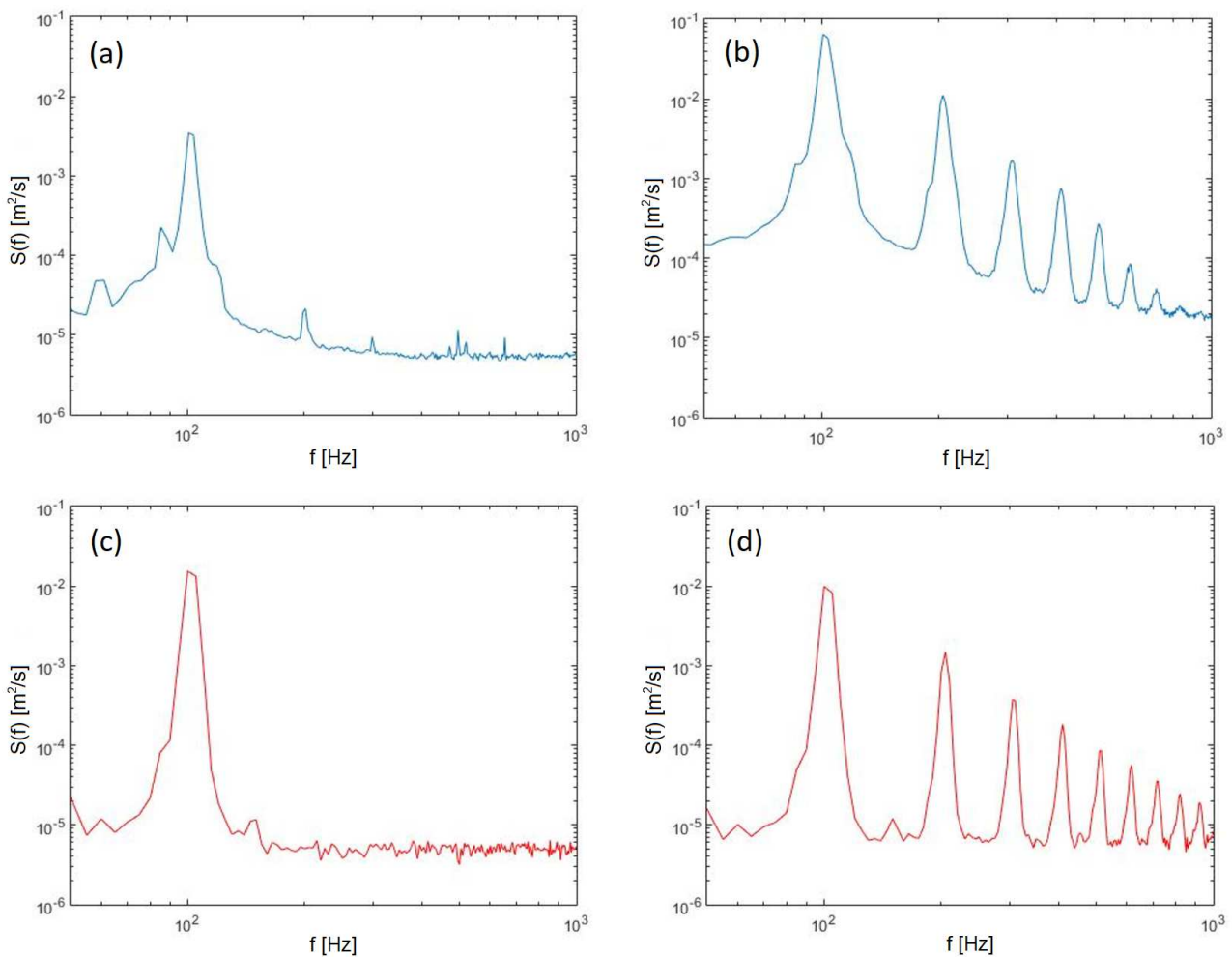


Fig. 11 Comparison of velocity power spectra at 1 mm (left) and 10 mm (right) from the rod edge. Blue: Measurements, video available at <https://doi.org/10.11583/DTU.12016827.v1>. Red: Computer simulations, video available at <https://doi.org/10.11583/DTU.12016869.v1>.

actions between injected energetic Fourier components through the downstream development of the velocity and power spectrum, as predicted from [20,21].

The authors hope that these results can be used by turbulence modelers to improve their methods, in particular the results on the generation and absorption of the harmonics of the initial injected frequency.

Acknowledgements Benny Edelsten is acknowledged for his assistance with the hot-wire experiments.

Conflict of interest

The authors declare that they have no conflict of interest.

References

1. Kolmogorov AN., “The local structure of turbulence in incompressible viscous fluid for very large Reynolds numbers”, *Proc. R. Soc. Lond. A*, (1991), 434, 9–13. <https://doi.org/10.1098/rspa.1991.0075> (1991)
2. Lvov V., Procaccia I., “Hydrodynamic turbulence: a 19th century problem with a challenge for the 21st century”. In: Boratav O., Eden A., Erzan A. (eds) *Turbulence Modeling and Vortex Dynamics*. Lecture Notes in Physics, vol 491. Springer, Berlin, Heidelberg. <https://doi.org/10.1007/BFb0105026> (1997)
3. Richardson LF., Lynch P., “Weather Prediction by Numerical Process”. 2nd edn. Cambridge: Cambridge University Press (Cambridge Mathematical Library). <https://doi.org/10.1017/CBO9780511618291> (2007)
4. Kraichnan RH., “The structure of isotropic turbulence at very high Reynolds numbers”, *Journal of Fluid Mechanics*. Cambridge University Press, 5(4), pp. 497–543, doi: 10.1017/S0022112059000362 (1959)
5. From <https://www.mashayek.com/research> collected on 15.03.2020

6. George WK., “A 50-Year Retrospective and the Future”, in: Whither Turbulence and Big Data in the 21st Century?, Springer International Publishing, https://doi.org/10.1007/978-3-319-41217-7_2 (2017)
7. Jossierand C., Le Berre M., Lehner T., Pomeau, Y., “Turbulence: Does Energy Cascade Exist?”. *Journal of Statistical Physics*, 167, 596–625. <https://doi.org/10.1007/s10955-016-1642-5> (2017)
8. Zhou Y., “Interacting scales and energy transfer in isotropic turbulence”, *Physics of Fluids A: Fluid Dynamics*, 5:10, 2511–2524, <https://doi.org/10.1063/1.858764> (1993)
9. Girimaji SS. and Zhou Y., “Spectrum and energy transfer in steady Burgers turbulence”, *Physics Letters A*, 202:4, 279–287, [https://doi.org/10.1016/0375-9601\(95\)00317-V](https://doi.org/10.1016/0375-9601(95)00317-V) (1995).
10. Yeung PK., Brasseur JG., Wang Q., “Dynamics of direct large-small scale couplings in coherently forced turbulence: concurrent physical- and Fourier-space views”, *Journal of Fluid Mechanics*. Cambridge University Press, 283, pp. 43–95. doi: 10.1017/S0022112095002230 (1995).
11. Brasseur JG., Corrsin S., “Spectral evolution of the Navier-Stokes equations for low order couplings of Fourier modes”, In: Comte-Bellot G., Mathieu J. (eds) *Advances in Turbulence*. Springer, Berlin, Heidelberg, pp. 152–162, (1987).
12. Domaradzki A., Rogallo RS., “Local energy transfer and nonlocal interactions in homogeneous, isotropic turbulence”, *Physics of Fluids A: Fluid Dynamics* 2, 413, <https://doi.org/10.1063/1.857736> (1990)
13. Ohkitani K., Kida S., “Triad interactions in a forced turbulence”, *Physics of Fluids A: Fluid Dynamics* 4, 794, <https://doi.org/10.1063/1.858296> (1992).
14. Laizet S., Nedić J., Vassilicos JC., “The spatial origin of $-5/3$ spectra in grid-generated turbulence”, *Physics of Fluids* 27, 065115, <https://doi.org/10.1063/1.4923042> (2015)
15. Yeung K., Brasseur JG., “The response of isotropic turbulence to isotropic and anisotropic forcing at large scales”, *Physics of Fluids A: Fluid Dynamics* 3, 884. <https://doi.org/10.1063/1.857966> (1991)
16. Vassilicos JC., “Dissipation in Turbulent Flows”, *Annual Review of Fluid Mechanics*, 47:1, 95–114, doi:10.1146/annurev-fluid-010814-014637 (2015).
17. Hunt JCR., Carruthers DJ., “Rapid distortion theory and the ‘problems’ of turbulence”, *Journal of Fluid Mechanics*. Cambridge University Press, 212, pp. 497–532. doi: 10.1017/S0022112090002075 (1990).
18. Mazellier N., Vassilicos JC., “Turbulence without Richardson-Kolmogorov cascade”, *Physics of Fluids* 22, 075101, <https://doi.org/10.1063/1.3453708> (2010)
19. Liao ZJ., Su WD., “Kolmogorov’s hypotheses and global energy spectrum of turbulence”, *Physics of Fluids* 27, 041701, <https://doi.org/10.1063/1.4916964> (2015)
20. Buchhave P., Velte CM., “Dynamic triad interactions and evolving turbulence spectra”, submitted for review, arXiv:1906.04756 [physics.flu-dyn] (2019)
21. Buchhave P., Velte CM., “A 1D Navier-Stokes Machine and its application to turbulence studies”, submitted for review, arXiv:2002.10184 [physics.flu-dyn] (2020)
22. Bo-Bin W., Gui-Xiang C., Xu C., Zhang ZS., “The Similarity of Non-local Triad Interactions in Energy Transfer of Isotropic Turbulence”, *Chinese Physics Letters*, 29:10, 104701, <https://doi.org/10.1088/0256-307X/29/10/104701> (2012).
23. Kellogg, RM., Corrsin, S., “Evolution of a spectrally local disturbance in grid-generated, nearly isotropic turbulence”, *Journal of Fluid Mechanics*. Cambridge University Press, 96(4), pp. 641669. doi: 10.1017/S0022112080002297 (1980).
24. Buchhave P., Velte CM., “Measurement of turbulent spatial structure and kinetic energy spectrum by exact temporal-to-spatial mapping”. *Physics of Fluids* 29, 085109, <https://doi.org/10.1063/1.4999102> (2017)
25. Lumley JL., “Stochastic Tools in Turbulence”, Academic Press, ISBN: 9780323162258 (1970).
26. Gibson MM., “Spectra of Turbulence at High Reynolds Number”, *Nature* 195, 1281–1283, <https://doi.org/10.1038/1951281a0> (1962)
27. Panchapakesan NR., Lumley JL., “Turbulence measurements in axisymmetric jets of air and helium. Part 1. Air jet”, *Journal of Fluid Mechanics*, Cambridge University Press, 246, pp. 197–223, doi: 10.1017/S0022112093000096 (1993)
28. Hussein HJ., Capp SP., George WK., “Velocity measurements in a high-Reynolds-number, momentum-conserving, axisymmetric, turbulent jet”, *Journal of Fluid Mechanics*. Cambridge University Press, 258, pp. 31–75. doi: 10.1017/S002211209400323X (1994).
29. Hinze JO., “Turbulence: An Introduction to Its Mechanism and Theory”, 2nd ed., Mcgraw-Hill College, (1975).
30. Ewing D., Frohnapfel B., George WK., Pedersen JM., Westerweel J., “Two-point Similarity in the Round Jet”, *Journal of Fluid Mechanics*, Cambridge University Press, 577, pp. 309330. doi: 10.1017/S0022112006004538 (2007).
31. Yaacob MR., Schlander RK., Buchhave P., Velte CM., “Experimental Evaluation of Kolmogorov’s $-5/3$ and $2/3$ Power Laws in the Developing Turbulent Round Jet”. *Journal of Advanced Research in Fluid Mechanics and Thermal Sciences*, 45(1), 14–21, (2018).
32. Yaacob MR., Schlander RK., Buchhave P., Velte CM., “Validation of improved laser Doppler anemometer (LDA) based on the fully developed turbulent round jet”. In M. Md Ghazaly, A. Zaki Shukor, G. Chin Kim, R. Ranom, Z. Rasin, M. Azri, A. Anas Yusof, S. Ahmad Radzi, N. Nordin, M. Bazli Bahar, S. Mohamad Shazali Syed Abdul Hamid, ... M. Arif Mohd Azman (Eds.), *Sh-proceeding of SEMA 2018 - Symposium on Electrical, Mecha-tronics and Applied Science 2018* (pp. 89–90). Universiti Teknikal Malaysia Melaka (UTeM).
33. Yaacob MR., Schlander RK., Buchhave P., Velte CM., “Mapping of the turbulent round jet developing region using a constant temperature anemometer (CTA)”. *Malaysian Journal of Fundamental and Applied Sciences*, (Special Issue on Natural Sciences and Mathematics (ESCon 2018)), 443–446. <https://doi.org/10.11113/mjfas.v14n0.1298>, (2018)
34. Bell JH., Mehtaz RD., “Contraction design for small low-speed wind tunnels”, Technical Report NASA-CR-177488, NAS 1.26:177488 (1988)
35. Capp SP., “Experimental Investigation of the Turbulent Axisymmetric Jet”. PhD-dissertation, University at Buffalo, May (1983)